Lagrangian statistics of pressure fluctuation events in homogeneous isotropic turbulence

Mehedi Bappy [iD], Pablo M. Carrica [iD], and Gustavo C. Buscaglia [iD]

View Online   Export Citation   CrossMark

ARTICLES YOU MAY BE INTERESTED IN

Lagrangian statistics of pressure fluctuation events in homogeneous isotropic turbulence

View Online   Export Citation   CrossMark

Mehedi Bappy,[1] 🆔 **Pablo M. Carrica,**[1] 🆔 and **Gustavo C. Buscaglia**[2] 🆔

AFFILIATIONS

[1] IIHR-Hydroscience and Engineering, The University of Iowa, Iowa City, Iowa 52242, USA
[2] Instituto de Ciências Matemáticas e de Computação, Universidade de São Paulo, São Carlos, Brazil

ABSTRACT

Homogeneous and isotropic turbulent fields obtained from two direct numerical simulation databases (with Re_λ equal to 150 and 418) were seeded with point particles that moved with the local fluid velocity to obtain Lagrangian pressure histories. Motivated by cavitation inception modeling, the statistics of events in which such particles undergo low-pressure fluctuations were computed, parameterized by the amplitude of the fluctuations and by their duration. The main results are the average frequencies of these events and the probabilistic distribution of their duration, which are of predictive value. A connection is also established between these average frequencies and the pressure probability density function, thus justifying experimental methods proposed in the literature. Further analyses of the data show that the occurrence of very-low-pressure events is highly intermittent and is associated with wormlike vortical structures of length comparable to the integral scale of the flow.

Published under license by AIP Publishing. https://doi.org/10.1063/1.5110265

I. INTRODUCTION

The study of pressure fluctuations in turbulent flows has been the subject of significant theoretical, numerical, and experimental work over more than eight decades. Over the years, much knowledge has been gained about the intensity of fluctuations, their scaling properties, their energy spectrum, and the probability density function (PDF) as well as about their spatial structure and their relation to other flow variables. The reader is referred, among others, to the works of George *et al.*[1] Pumir,[2] Cao *et al.*[3] Gotoh and Rogallo,[4] and the references therein for further details.

Pressure fluctuations have important practical consequences in many physical situations since they intervene in the forces exerted by the fluid on adjacent and immersed bodies and are also key to acoustic noise. The specific motivation of the study reported herein is the phenomenon of incipient cavitation in turbulent liquid flows, which is a macroscopic consequence of pressure fluctuations on microscopic bubbles (or *nuclei*) present in the liquid.[5,6] Although the dynamics of cavitation bubbles has been well established following the pioneering work of Plesset,[7] accurate prediction of cavitation inception in technologically relevant flows remains a challenge.[8,9]

A seminal work on cavitation inception in turbulent flows was published in 1979 by Arndt and George.[10] It puts forward the main ingredients for turbulence-induced inception: that the cavitation nuclei are subject to pressure fluctuations as measured in a *Lagrangian frame* and that (a) the pressure must dip below a critical level (p_{cav}, the *cavitation pressure*, also called *Blake threshold*[11]) and (b) the low pressure must persist below the critical level for a time that exceeds the time scale for bubble growth. The picture has been confirmed and enriched over the years by several authors,[12–15] including the role of coherent structures and the possibility of using incipient cavitation bubbles as pressure sensors.

Typically, cavitation inception is defined by the inception cavitation index $\sigma_i = (p_{\mathrm{ref},i} - p_{\mathrm{cav}})/(\frac{1}{2}\rho U^2)$, where $p_{\mathrm{ref},i}$ is the value of the reference pressure of the flow at which cavitating nuclei first become *observable*, ρ is the liquid's density, and U is the global velocity scale. By observable, it is meant that the *frequency* of cavitation events growing bubbles to a large enough size is high enough to be experimentally detectable. In view of criteria (a) and (b) above, inception modeling thus requires knowledge about *the frequency ζ at which random turbulent fluctuations take the pressure, as experienced by the minute nuclei transported by the flow, below p_{cav} for long enough time.* Such knowledge is, however, not as yet available

in the literature. The purpose of this contribution is to provide data about ζ in the simplest turbulent flow, homogeneous isotropic turbulence (HIT). As such, the results are related to the so-called *homogeneous nucleation* of cavitation, in which the events take place far away from walls. To address *heterogeneous nucleation*, one should increase at least one step further the complexity of the flow and consider boundary layer turbulence.

The pressure PDF in HIT is known to be negatively skewed and exhibit an exponential tail at very low pressures.[2–4] On the basis of physical intuition, several authors have argued that the frequency $\zeta(\delta p)$ of pressure fluctuations below δp should also exhibit an exponential tail for large and negative δp.[10,12,14] Mathematically, this is far from obvious. In fact, consider a $p(t)$ that exhibits logarithmic pulses of the form $\ln(t - t_i)$, where $t_1, t_2, \ldots$ are random times which arise with average frequency f. It is easy to check that in such a case PDF(p) has an exponential tail for $p \ll 0$. However, the frequency $\zeta(\delta p)$ is not exponential, as it equals f for any (sufficiently negative) δp. The temporal structure of the pressure excursions is thus crucial in determining the statistics of occurrence of low pressure events.

Having in mind cavitation modeling, in this investigation, we perform Lagrangian sampling of two Direct Numerical Simulation (DNS) databases counting events at which the particles go below some given pressure threshold δp for a longer time than some given minimum duration $d \geq 0$. Note that each excursion, even if the pressure dives well below δp for a time much greater than d, is counted as a single event. The rationale behind this is that, if the given δp and d are likely to produce cavitation of the particle (nucleus), then the gaseous phase will violently grow and increase the local pressure so that no similar event will take place within the same pressure excursion. The results obtained from our Lagrangian counting experiments confirm the exponential dependence $\zeta(\delta p) \simeq C \exp(\beta \delta p)$ for $\delta p \ll 0$. The factors C and β are retrieved by fitting the data. We also address the random structure of the pressure fluctuation events by building the PDF of interarrival times. It shows that low-pressure events do not behave as a Poisson process, exhibiting a marked burstiness that increases as δp becomes more negative. It is appropriate to point out that, since the tracking method does not incorporate any relative velocity between the Lagrangian particles and the fluid, the results only apply to the smallest cavitation nuclei.

II. DEFINITIONS AND METHODS

Two databases containing Direct Numerical Simulation (DNS) results of Forced Homogeneous Isotropic Turbulence (FHIT) were queried. They consist of fully resolved numerical solutions of the incompressible Navier-Stokes equations in a periodic domain, with forcing applied to a narrow band of low wavenumber modes in such a way that a statistically steady flow develops.

The DNS results are time series of velocity and pressure spatial fields with zero mean from which statistical averages of kinetic energy $\langle K \rangle$ and viscous dissipation $\langle \epsilon \rangle$ were computed. From these values, the basic scales characterizing each flow were defined as

$$\begin{cases} \text{Velocity scale:} & u' = \sqrt{\frac{2\langle K \rangle}{3}}, \\ \text{Length scale:} & \lambda = u'\sqrt{\frac{15\nu}{\langle \epsilon \rangle}}, \end{cases} \quad (1)$$

where ν is the kinematic viscosity and unit density is used. The length scale so defined is the Taylor length microscale. With these two basic scales, all variables were rescaled (nondimensionalized), dividing velocities by u', lengths by λ, pressures by $\rho u'^2$, times by λ/u', etc. All reference to the DNS data made throughout this article concerns the scaled (dimensionless) variables. In particular, the scaled velocity field $\mathbf{u}$ satisfies

$$\langle \|\mathbf{u}\|^2 \rangle = 3, \qquad \langle \|\nabla \times \mathbf{u}\|^2 \rangle = 15. \quad (2)$$

The nondimensional parameter that characterizes the flow is the Reynolds number $Re_\lambda = u'\lambda/\nu$. Two values were considered: $Re_\lambda = 150$, obtained from the database maintained by Jiménez and coworkers at Univ. Politécnica Madrid,[16] and $Re_\lambda = 418$, obtained from the Johns Hopkins Turbulence Databases.[17–19]

Note that, under this scaling, the Kolmogorov scales[20] are given by

$$\begin{cases} \text{Length:} & \eta_K = 15^{-\frac{1}{4}} Re_\lambda^{-\frac{1}{2}} = 0.508\, Re_\lambda^{-\frac{1}{2}}, \\ \text{Velocity:} & u_K = 15^{\frac{1}{4}} Re_\lambda^{-\frac{1}{2}} = 1.968 Re_\lambda^{-\frac{1}{2}}, \\ \text{Time:} & \tau_K = 15^{-\frac{1}{2}} = 0.2582. \end{cases} \quad (3)$$

Notably, τ_K is independent of Re_λ. The Reynolds number based on the Kolmogorov length is then $Re_\eta = u'\eta_K/\nu = 15^{-\frac{1}{4}} Re_\lambda^{\frac{1}{2}} = 0.508 Re_\lambda^{\frac{1}{2}}$.

The Lagrangian trajectories are computed by numerically solving the equation

$$\frac{d\mathbf{r}}{dt}(t) = \mathbf{u}(\mathbf{r}(t), t) \quad (4)$$

from time $t = 0$ to $t = T$, with initial condition $\mathbf{r}(0) = \mathbf{X}$, for a large number M of initial positions, i.e., $\mathbf{X} \in \mathcal{X} = \{\mathbf{X}^1, \mathbf{X}^2, \ldots, \mathbf{X}^M\}$. The adopted time-integration method is a Runge-Kutta scheme of order ≥ 2, with a time step smaller than the Kolmogorov time scale ($\Delta t < 0.05$). The required spatial interpolation was accomplished using Lagrangian polynomial interpolants of degree three or greater, depending on the case.

Along the set of computed trajectories, several statistical estimates were computed by averaging over the Lagrangian samples (parameterized by the set $\mathcal{X}$ of initial positions) and over time. For these estimates to be meaningful, recommended practices were followed.[21] The initial positions were uniformly distributed over the simulation domain, keeping them at least 2.5 grid spacings apart. The integration time T extended over several eddy turnover times. Specifically, the $Re_\lambda = 150$ field (resolution 256^3, time step 0.043) was sampled with $M = 10^6$ particles during a time $T = 869.1$ (114 turnover times). The $Re_\lambda = 418$ field (resolution 1024^3, time step 0.012), on the other hand, was sampled with $M = 4 \times 10^5$ particles during a time $T = 60.7$, which corresponds to 5 turnover times.

In incompressible turbulence, Lagrangian averages of spatial quantities (e.g., kinetic energy, enstrophy, etc.) coincide with Eulerian averages. Due to the finite number of Lagrangian particles and the finite simulation time, especially in the case with $Re_\lambda = 418$, the estimates obtained by averaging over the particles and over time are not exact. The difference of our estimates with Eulerian averages can be used as a simple test of statistical significance. The error in the

rms values of velocity and vorticity was smaller than 2%, value recommended by Yeung,[21] providing some validation of our sampling procedure.

The Lagrangian "Taylor" time scale of a variable Y is defined as[21]

$$\tau_Y = \left[\frac{\mathrm{Var}(Y)}{\mathrm{Var}(DY/Dt)} \right]^{\frac{1}{2}}, \tag{5}$$

where $\mathrm{Var}(\cdot)$ denotes the variance of the corresponding quantity and D/Dt is the material derivative. The Lagrangian autocorrelation function of a variable Y with zero mean is defined by

$$\rho_Y(s) = \frac{\langle Y(\mathbf{r}(t),t)Y(\mathbf{r}(t+s),t+s) \rangle}{\mathrm{Var}(Y)}. \tag{6}$$

The Lagrangian integral time scale of Y, denoted by $\mathcal{T}(Y)$, is given by

$$\mathcal{T}_Y = \int_0^{+\infty} \rho_Y(s)\, ds. \tag{7}$$

All the statistical averages in the previous and forthcoming definitions are of course replaced by estimates computed over the numerical approximation of the sampled trajectories.

Finally, the occurrence of low pressure events was investigated as follows: Some negative pressure values p_- were chosen, namely, -2, -2.05, -2.1, etc. Note that these correspond to nondimensional fluctuations, since $\langle p \rangle = 0$. For a given value of p_-, a Lagrangian particle was defined as undergoing a *low-pressure event with threshold* p_- that starts at time t_{start} if its pressure satisfies $p(t_{\mathrm{start}}) = p_-$ and $Dp/Dt(t_{\mathrm{start}}) < 0$. The end of the event is defined as the first time t_{end} such that $p(t_{\mathrm{end}}) = p_-$ and $Dp/Dt(t_{\mathrm{end}}) > 0$. The *duration* of the event is defined as $t_{\mathrm{end}} - t_{\mathrm{start}}$.

In this way, given m particles evolving in a turbulent field, a stochastic *counting process* $n(p_-, d, t)$ can be defined as the number of low-pressure events (with threshold p_- and duration $t_{\mathrm{end}} - t_{\mathrm{start}} > d$) that have $0 < t_{\mathrm{start}} < t$. For each threshold p_- and each minimum duration d, the number $n(p_-, d, T)$ of events was computed from the time history of the M Lagrangian particles that are traced over the time T of the simulation. From this, we computed an estimate for the rate of such events as

$$\zeta(p_-, d) \simeq \frac{n(p_-, d, T)}{MT}. \tag{8}$$

An analogous processing was carried out for high-pressure events, denoting the (positive) threshold by p_+.

III. RESULTS

A. Basic statistics

We first report some basic statistical quantities obtained from the computed Lagrangian pressure histories. These include the pressure PDFs shown in Fig. 1, together with the quantities summarized in Table I.

The results for $\mathrm{Var}(p)$ are similar to those of Gotoh and Rogallo,[4,22] who reported a value of about 0.9 at $Re_\lambda = 39$ which decreased to about 0.7 at $Re_\lambda = 172$. Cao *et al.*[3] reported
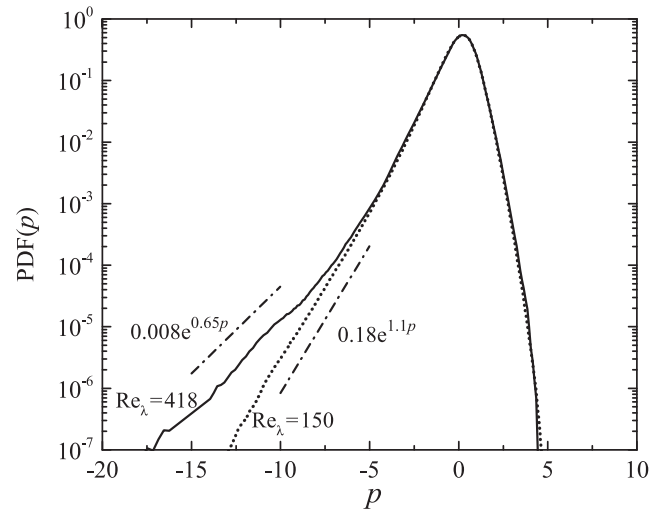

FIG. 1. Pressure PDFs obtained from the Lagrangian data at $Re_\lambda = 150$ and 418. The dashed-dotted lines depict the fitted exponentials of Eq. (9), shifted for clarity.

TABLE I. Basic statistics of the computed Lagrangian pressure histories.

Quantity	Symbol	$Re_\lambda = 150$	$Re_\lambda = 418$
Variance of p	$\mathrm{Var}(p)$	0.78	0.82
Variance of Dp/Dt	$\mathrm{Var}(Dp/Dt)$	1.48	0.36
Time microscale	τ_p	0.73	1.51
Integral time scale	$\mathcal{T}_p$	2.30	6.21

$\mathrm{Var}(p) = 0.883$ at $Re_\lambda = 131$, while Pumir[2] obtained $\mathrm{Var}(p) \simeq 1$ for $21.6 \le Re_\lambda \le 77.5$. Lagrangian Taylor and integral time scales for pressure are not available in the literature, nor is the Lagrangian pressure autocorrelation function, which is shown in Fig. 2.
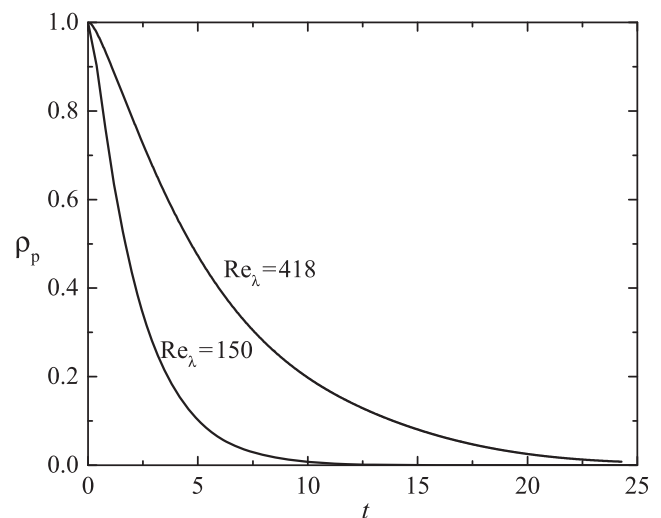

FIG. 2. Lagrangian pressure autocorrelation functions at $Re_\lambda = 150$ and 418.

The pressure PDFs exhibit the (approximately) exponential tails previously reported by Pumir[2] and Cao et al.[3] Specifically, the data can be fitted by

$$\text{PDF}(p) \simeq \begin{cases} 0.18 \exp(1.1\,p) & \text{for } Re_\lambda = 150,\ -13 \le p \le -5 \\ 0.008 \exp(0.65\,p) & \text{for } Re_\lambda = 418,\ -17 \le p \le -7 \end{cases}. \quad (9)$$

B. Average frequency of pressure fluctuation events

The main novel results in this contribution are the values of $\zeta(p_-, d)$ as depicted in Fig. 3. Note that ζ is an average frequency of events *per particle*. An estimate of its relative statistical error can be
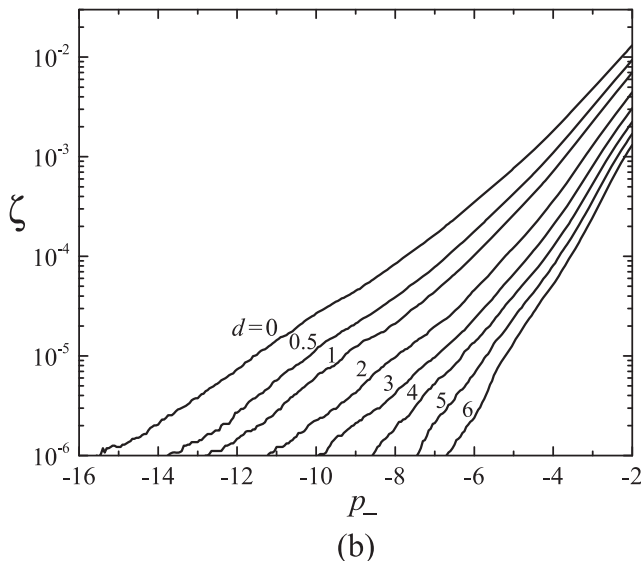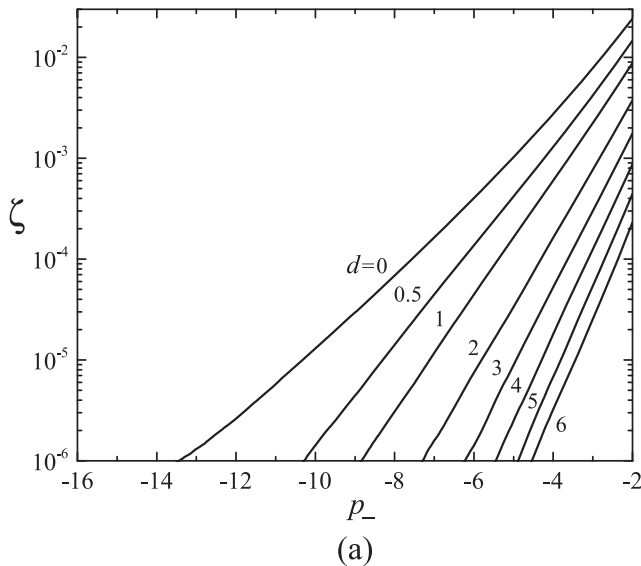
FIG. 3. Nondimensional frequency $\zeta(p_-, d)$ of low-pressure events as a function of the threshold pressure p_- for several values of the minimum duration $d = 0, 0.5, 1, \ldots$. Results at (a) $Re_\lambda = 150$ and (b) $Re_\lambda = 418$.
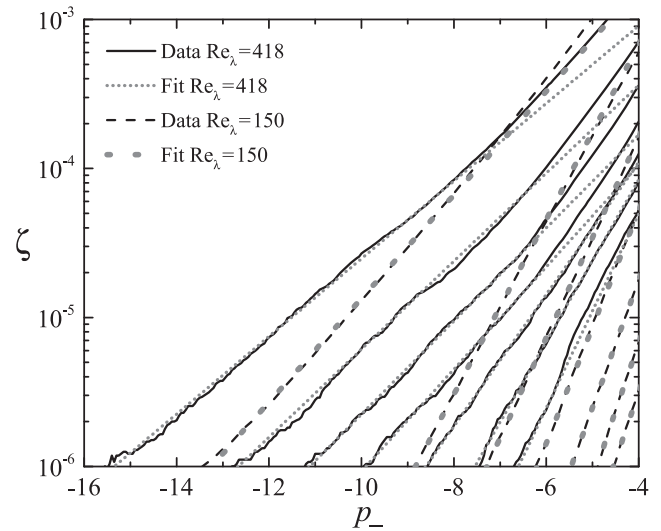
FIG. 4. $\zeta(p_-, d)$ for $d = 0, 1, \ldots, 6$, for both values of Re_λ, and their exponential fits.

obtained as $1/\sqrt{n(p_-, d, T)}$ for each computed value. This makes the relative error of ζ to be proportional to $\zeta^{-1/2}$, with a proportionality constant of 3×10^{-5} for the $Re_\lambda = 150$ simulation and of 2×10^{-4} for the $Re_\lambda = 418$ one. No values of ζ below 10^{-6} are reported because for this value the relative statistical error is already at 20% for the higher Re.

A typical use of these data would be as follows: Consider a volume V of fluid in a (homogeneous, isotropic) turbulent flow characterized by given values of u', λ, and Re_λ, and assume that the fluid contains some concentration Z of small particles (per m^3) in suspension. Then, $F = ZV\zeta(p_-, d)u'/\lambda$ is the expected frequency (in events/second) with which the suspended particles will undergo negative pressure fluctuations below $\rho u'^2 p_-$ (in Pa) that last more than $d\lambda/u'$ (in s) within the volume V. Of course, for this to hold, the quantity $\zeta(p_-, d)$ must be evaluated at the flow's Re_λ.

Going back to Fig. 3, note that for any minimum duration d the average frequency is approximately exponential in p_-, i.e., $\zeta(p_-)$

TABLE II. Constants C and β of the exponential fits of the data, for low-pressure events of duration greater or equal than d and for the two datasets ($Re_\lambda = 150$ and 418). The quality of the fits can be appreciated in Fig. 4.

Min. duration (d)	$Re_\lambda = 150$		$Re_\lambda = 418$	
	C	β	C	β
0	0.04	0.80	0.010	0.60
1	0.15	1.35	0.0055	0.68
2	0.08	1.55	0.003	0.72
3	0.07	1.80	0.0025	0.79
4	0.047	1.97	0.0065	1.02
5	0.03	2.10	0.0125	1.25
6	0.014	2.10	0.022	1.50

$\simeq C \exp(\beta p_-)$, with C and β depending on d and on Re_λ. In fact, some upward concavity can be observed in the semilog plots for the higher values of p_- (milder pressure fluctuations), but for lower values the plots closely follow straight lines. This can be more easily seen in Fig. 4, in which all plots of $\zeta(p_-, d)$ corresponding to $d = 0, 1, 2, \ldots,$ 6 for both values of Re_λ have been put together simultaneously with their exponential fits.

The fitted values of C and β are listed in Table II. Most relevant is the parameter β, i.e., the slope in the semilog plots. A smaller β implies that, as the threshold is lowered, the average rate of excursions below the threshold decreases more slowly. For any minimum

duration of the excursions, β is smaller for the higher Reynolds number. This is consistent with the pressure PDFs, which also show that lower pressures become more probable at higher Re_λ, with exponential tails that behave as $\exp(\gamma p_-)$, with $\gamma = 1.1$ at $Re_\lambda = 150$ and $\gamma = 0.65$ at $Re_\lambda = 418$ (see Fig. 1).

By direct inspection of Table II, one notices that γ is, for both Re_λ, close to the parameter β that corresponds to events of minimum duration d between 0 and 1 (i.e., between zero and roughly four Kolmogorov time scales). The experimental consequences of this are quite interesting. Assume that, as proposed by LaPorta et al.,[14] one uses the gas nuclei in a liquid as pressure sensors and measures the average rate of cavitation events as a function of the (variable) reference pressure p_{ref} of the flow. Then, *if the nuclei's*
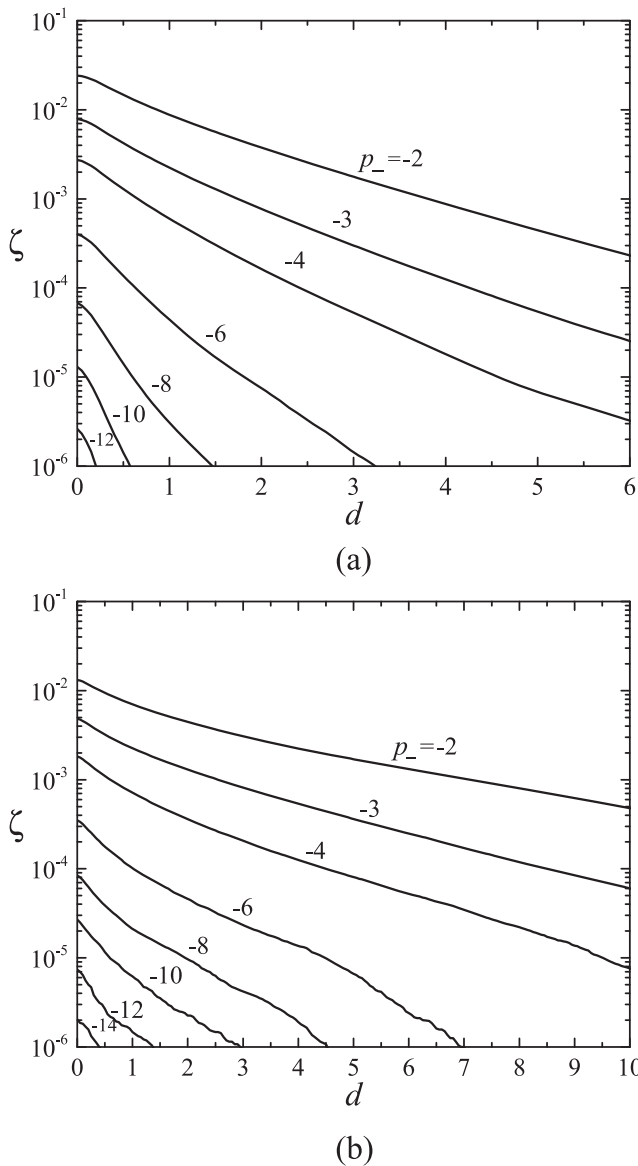

FIG. 5. Nondimensional frequency $\zeta(p_-, d)$ of low-pressure events as a function of minimum duration d for several values of the threshold pressure ($p_- = -2, -3, -4, \ldots$). Results at (a) $Re_\lambda = 150$ and (b) $Re_\lambda = 418$.
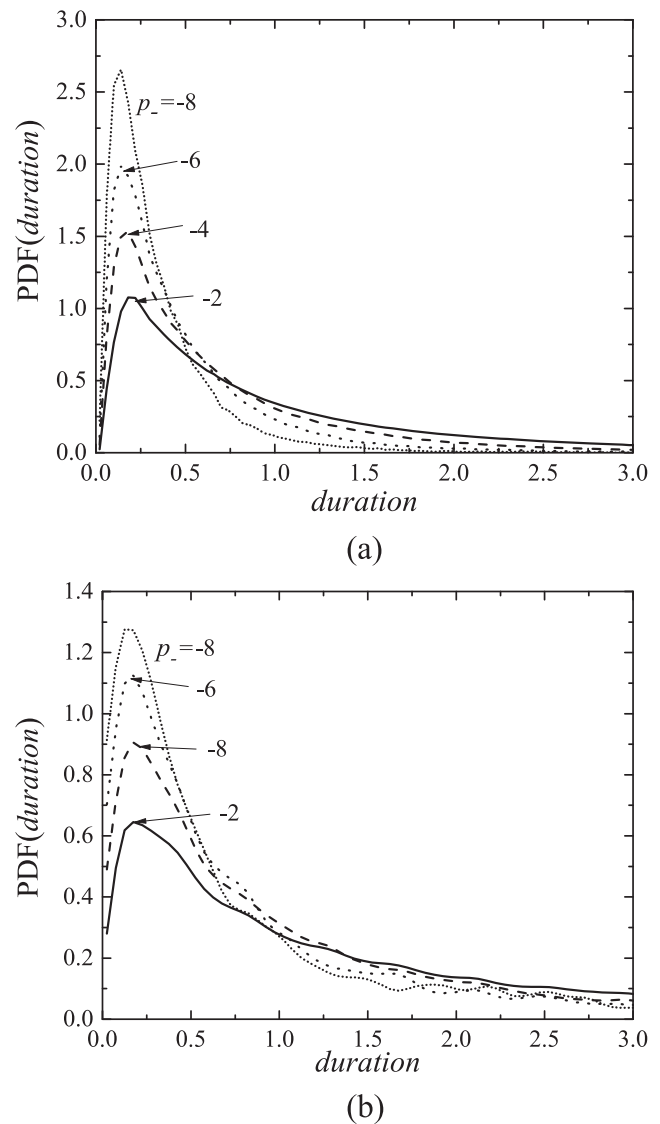

FIG. 6. PDFs of the duration of the low-pressure events for several values of the threshold pressure ($p_- = -2, -4, -6, -8$). Results at (a) $Re_\lambda = 150$ and (b) $Re_\lambda = 418$.

reaction time is smaller than a few Kolmogorov time scales, the curve *cavitation rate* vs $(p_{cav} - p_{ref})$ will be approximately proportional to $\int_{-\infty}^{p_{cav} - p_{ref}} \text{PDF}(p)\, dp$ and thus, since $\text{PDF}(p)$ is exponential, to $\text{PDF}(p_{cav} - p_{ref})$ itself. This has been argued in the literature by several authors[10,12,14] on the basis of physical intuition and is herein rigorously confirmed. Note that the short reaction time of the nuclei is crucial for the proportionality $\zeta(p_-) \sim \text{PDF}(p_-)$ to hold. If the reaction time is larger than, say, $20\tau_K$ (corresponding to $d \simeq 5$), the dependence of the cavitation rate with pressure will largely differ from that of the pressure PDF. It is worth mentioning that the values of β inferred by LaPorta *et al.*,[14] which were in the range 0.14–0.22 for Re_λ between 1658 and 1880, suggest that β keeps decreasing with Re_λ in much the same way as observed from the DNS databases studied here.

The dependence of ζ with the minimum duration d of the events is depicted in Fig. 5. An approximately exponential decay of ζ with d is observed for d greater than a few τ_K (say, $d > 0.5$), with a logarithmic slope that becomes more negative as the threshold p_- is lowered. For any p_-, the average rate of long events increases significantly with Re_λ.

It is informative to complement the previous results with further analysis of the distribution of the duration $(t_{end} - t_{start})$ of the events corresponding to each threshold p_-. The corresponding PDFs are shown in Fig. 6. It is observed that the peak of the PDF is always about 2/3 of τ_K and that the PDFs for each p_- have longer tails for the larger Re_λ. As p_- decreases, the distribution becomes narrower, i.e., events that last longer than τ_K become increasingly improbable. The means and medians of these PDFs are shown as functions of p_- in Fig. 7. They increase significantly with Re_λ, contrary to what happens with the peak of duration PDFs.

For the purpose of both completeness and comparison, let us close this section with plots of $\zeta(p_+, d)$, corresponding to *positive* pressure fluctuations. They are shown in Fig. 8. It is evident that positive pressure excursions are much more rare than negative ones, a result that is consistent with the rapid decay of the positive side of
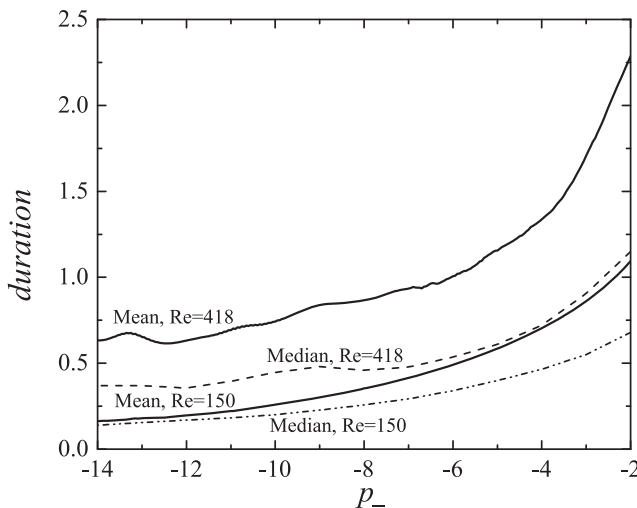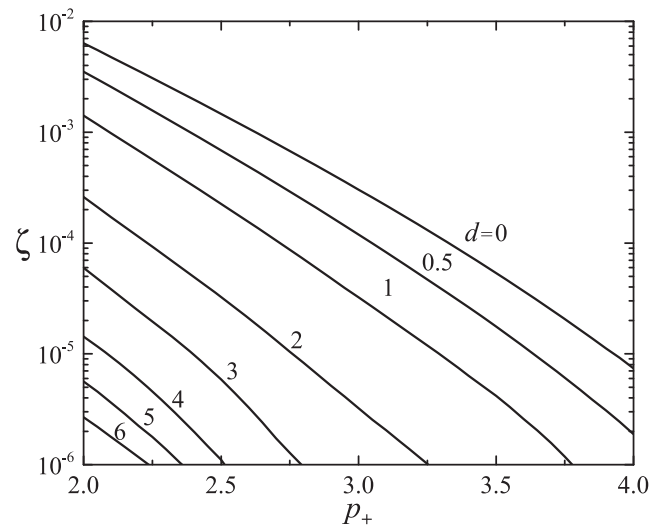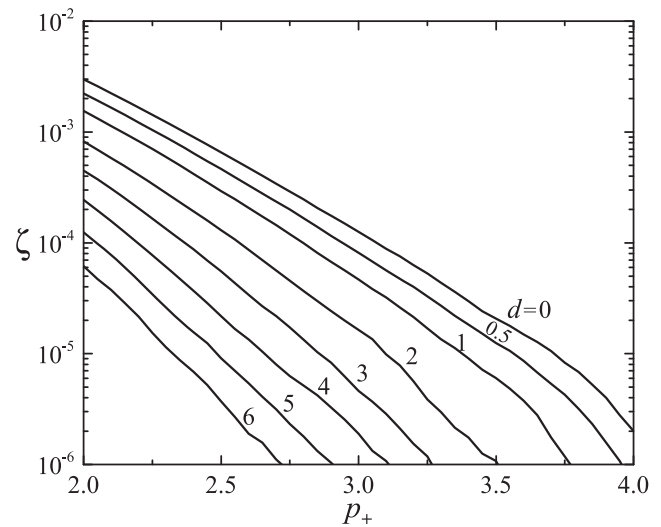

(a)

(b)

FIG. 8. Obtained values of nondimensional frequency $\zeta(p_+, d)$ of high-pressure events as a function of the threshold pressure p_+ for several values of the minimum duration d. Results at (a) $Re_\lambda = 150$ and (b) $Re_\lambda = 418$.

the pressure PDF. For minimum duration $d = 0$, the rate of events does not change much with Re_λ, but for events significantly longer than 10 Kolmogorov time scales ($d > 2.58$), the nondimensional frequency for $Re_\lambda = 418$ is much greater than that for $Re_\lambda = 150$, by an order of magnitude or more.

C. Randomness of low-pressure fluctuations

The occurrence of low-pressure fluctuations (of threshold p_- and minimum duration d) in a turbulent flow is certainly a random process. Its stochastic properties can be investigated looking at the *arrival process* formed by the (monotone increasing)

FIG. 7. Mean and median duration of the low-pressure events as functions of the threshold pressure p_-.

sequence $t_{start}^{(1)}, t_{start}^{(2)}, \ldots$, where $t_{start}^{(i)}$ is the starting time of the ith event. This generates the stochastic process of *interarrival times*, $D_i = t_{start}^{(i+1)} - t_{start}^{(i)}$. If m random particles are seeded into the flow, then by definition the average interarrival time satisfies $\overline{D} = 1/(m\zeta(p_-, d))$. A totally random arrival process (Poisson process) exhibits an exponential distribution for D, i.e.,

$$\text{PDF}(D) = \frac{1}{\overline{D}} \exp\left(-\frac{D}{\overline{D}}\right). \tag{10}$$

Whether the sequence of low-pressure events is a Poisson process or not can thus be assessed by inspecting the PDF of interarrival times. This PDF cannot be built from the raw data consisting of all

events undergone by the M particles because of the temporal resolution limit imposed by the simulation time step. For example, for the case of events with $p_- = -2$ and $d = 0$, the total number of such events recorded was 2.11×10^7 for the simulation at $Re_\lambda = 150$ ($M = 10^6$) and 3.43×10^5 for that at $Re_\lambda = 418$ ($M = 4 \times 10^5$). Meanwhile, the number of simulated time steps is 20 000 and 5000, respectively. This makes the interarrival times to be much smaller than the time step and thus poorly resolved.

The procedure adopted to build $PDF(D)$ was as follows: From the M particles in the simulation, batches of m particles were extracted at random, selecting the number m such that $\overline{D}$ equals 100 simulation time steps. For each batch, the interarrival times were computed, and PDF(D) was obtained averaging the histograms of 50 000 such batches.

The results considering events of any duration ($d = 0$) for each pressure threshold are shown in Fig. 9, where we plot $\overline{D}\,\text{PDF}(D)$ as a function of $D/\overline{D}$. Also shown is the exponential distribution $\exp(-D/\overline{D})$ which would correspond to a Poisson process. Analogous PDFs can be built for other values of d, but they are not shown since they are quite similar.

The first immediate observation from the plots of PDF(D) is that low-pressure events do not take place as a totally random, Poisson process that would entail an exponential PDF. The semilog-plots of the PDFs of interarrival times exhibit an upward concavity, or "heavy tail," which becomes more prominent as the threshold p_- is decreased. This heavy tail is characteristic of processes that exhibit *burstiness*, for which a popular quantitative measure in the literature is the "burstiness parameter"[23] defined by

$$B = \frac{\sigma(D) - \overline{D}}{\sigma(D) + \overline{D}}, \tag{11}$$

where $\sigma(D)$ is the standard deviation of D. Note that $B = -1$ for a periodic process ($\sigma(D) = 0$), $B = 0$ for a Poisson process ($\sigma(D) = \overline{D}$), and $B = 1$ for a highly bursty process ($\sigma(D) \gg \overline{D}$). The graphs of B vs p_- fixing the minimum duration to $d = 0$ are shown in
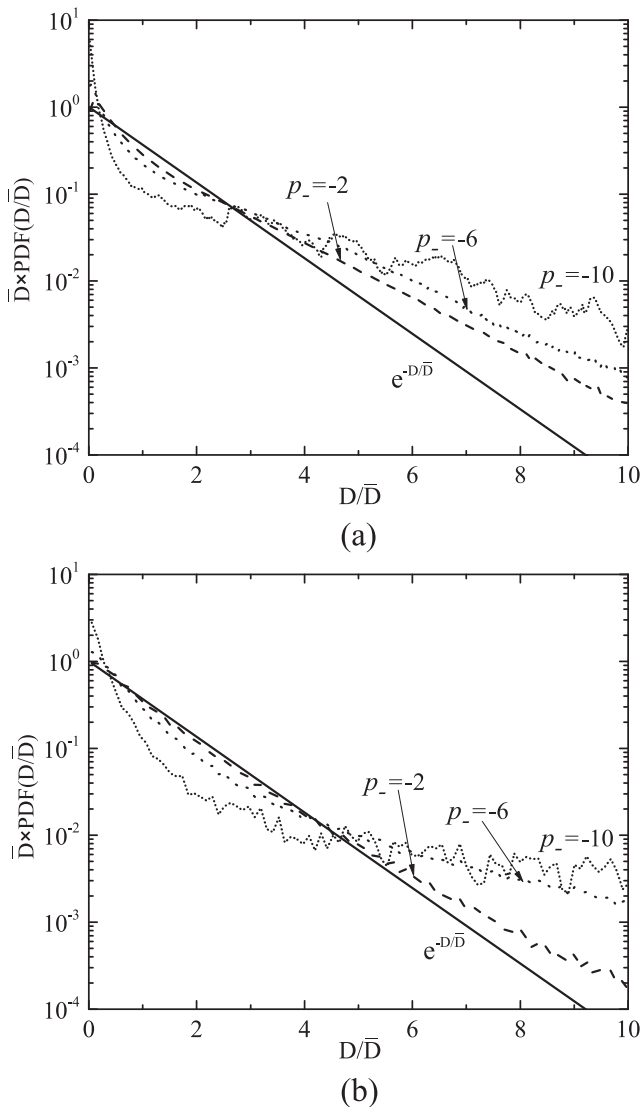

FIG. 9. PDF of the interarrival times of low pressure events of any duration ($d = 0$) for different thresholds p_-. The exponential corresponding to a Poisson process is also plotted for comparison. Results at (a) $Re_\lambda = 150$ and (b) $Re_\lambda = 418$.
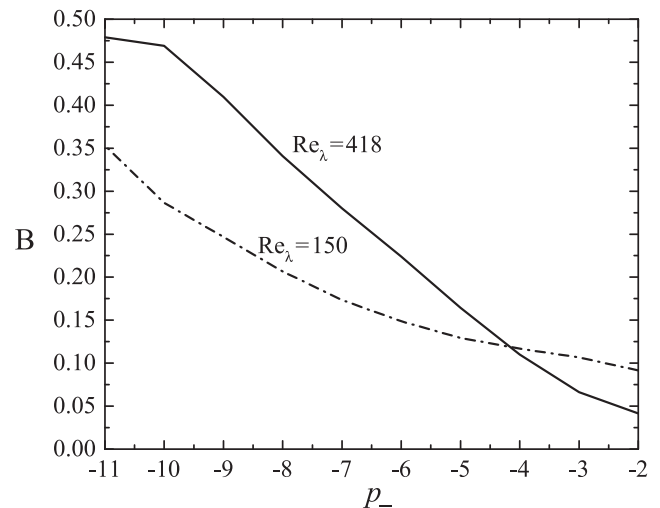

FIG. 10. Burstiness parameter of the low-pressure events as a function of the threshold pressure p_- for the two Re_λ considered.
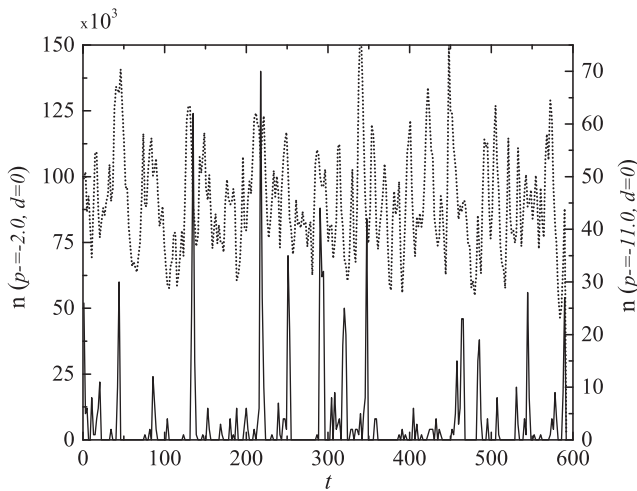
FIG. 11. Number of events that start within a time bin (size of the bin: 50 time steps) as a function of time. The plots correspond to events of threshold $p_- = -2$ (dotted line) and -11 (solid line), with minimum duration $d = 0$, as recorded in the $Re_\lambda = 150$ simulation.

Fig. 10 for both Re_λ considered. Clearly, the low-pressure events are more bursty for larger fluctuations (more negative p_-). To visualize this, in Fig. 11, we plot, as a function of time, the number of events that start in temporal bins of 50 time steps for $p_- = -2$ and $p_- = -11$ in the simulation with $Re_\lambda = 150$. The number of events per bin with threshold -2 oscillates moderately around its mean

value, while that with threshold -11 is most of the time near zero with intermittent bursts that reach 30 or more events per bin. It is remarkable that burstiness parameters of value 0.3 and higher are observed. Such values are not frequent in natural phenomena and can be found in highly intermittent human activities such as e-mail sending.[23]

The high burstiness of very-low-pressure events is an indication of large flow structures being involved in them such that when one of these structures appears, many particles go through it and bursts of events take place. This picture is consistent with the intermittent structures of intense vorticity, or *worms*, first described by Jiménez *et al.*,[24] which have lengths of the order of the integral scale of the flow. To confirm this, we looked at the pressure isosurfaces of the $Re_\lambda = 418$ simulation, for which a burst of low-pressure events takes place for nondimensional times between 6 and 18 (the burst thus lasts about 46 Kolmogorov time scales). The isosurfaces are shown in Fig. 12 at some selected instants. The lightest surfaces, corresponding to $p = -2$, are present in all snapshots as expected from the low value of B for $p_- = -2$. At time $t = 6.4$, a vortical structure develops, which is most evident at the peak of the burst (between $t = 9.1$ and 11.8, third and fourth frames in the figure). It is within this structure that very low pressures (-8 or lower) occur and affect numerous Lagrangian particles. By time 14.4, this structure is dissolving away, and after the burst, at $t = 25.1$, the flow has recovered an isosurface pattern similar to the one observed before the burst. We have checked that the vertical low-pressure structure is indeed a high vorticity region, and its shape and length are in agreement with the intermittent worms reported in the literature (note that the integral length scale for this flow is 12.1, roughly 1/5 the box edgelength).[24]
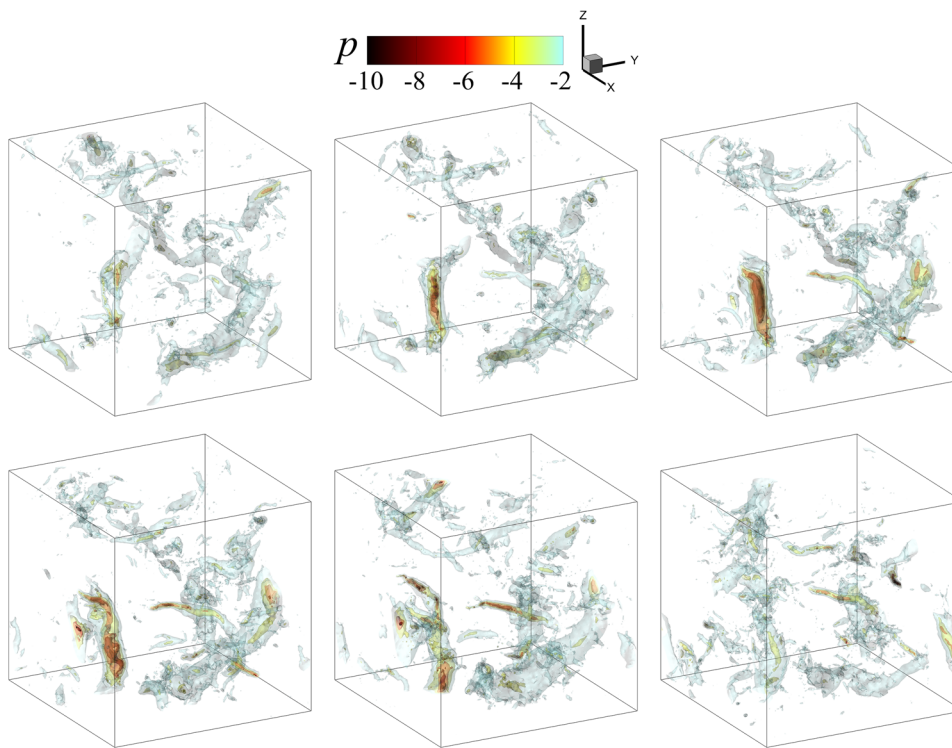

FIG. 12. Pressure isosurfaces of values $p = -2, -4, -6, -8,$ and -10 during a burst of very-low-pressure events. The corresponding times are, from left to right and top to bottom, $t = 3.8, 6.4, 9.1, 11.8, 14.4,$ and 25.1. The size of the periodic box is 55.6, and the integral scale is 12.1.

IV. CONCLUSIONS

Motivated by cavitation inception modeling, this work reports some Lagrangian statistics of the pressure field in forced homogeneous isotropic turbulence. It is clear that for a cavitation nucleus to grow up to detectable size, a pressure fluctuation that takes it to sufficiently low pressures for long enough time is necessary. However, the frequency of such low-pressure events was not available in the literature and is first reported herein for two values of Re_λ, namely, 150 and 418. The main result consists of the average frequency $\zeta(p_-, d)$ with which a Lagrangian particle undergoes a fluctuation that takes its pressure below some threshold p_- for a time longer than some minimum duration d. This average frequency, for any d, is observed to have an exponential tail [i.e., to behave as $\sim C \exp(\beta p_-)$] toward very low pressure thresholds. Furthermore, the value of the logarithmic slope β that corresponds to $d \simeq 0$ is roughly coincident with that of the exponential tail of the pressure PDF. The PDF of the duration of low-pressure events is also reported, which shows that the most probable duration is smaller than the Kolmogorov time scale and quite insensitive to p_- for both Re_λ considered. On the other hand, the mean and median duration of the pressure excursions grow significantly with Re_λ and depend strongly on p_- but only for moderate values of this variable. The analysis of the interarrival times between low-pressure events shows that their occurrence departs from that of a totally random homogeneous stochastic process (Poisson process). This departure becomes more and more accentuated as the threshold p_- is lowered. The distribution of interarrival times is heavy-tailed, indicative of a bursty process. In fact, a quantitative indicator of burstiness was computed, yielding values indicative of a highly intermittent process. This suggests that the bursts of low-pressure events are associated with intermittent large-scale vortical structures,[24] as confirmed by examination of the pressure isosurfaces at the time of the bursts.

The reported results provide useful quantitative data to predict the frequency, intensity, and duration of pressure fluctuations experienced by very small particles that are passively transported by a turbulent flow. They can be used, for example, to inform modern models of numerical cavitation.[25–27] The behavior at higher Reynolds numbers and in other turbulent flows should certainly be explored to gain further understanding. Also, the relative velocity that develops between non-neutrally buoyant particles of finite size and the surrounding liquid could attract bubbles toward vortex cores and strongly affect the computed frequencies. These issues are the subject of ongoing work.

ACKNOWLEDGMENTS

REFERENCES

[1] W. George, P. Beuther, and R. Arndt, "Pressure spectra in turbulent free shear flows," J. Fluid Mech. **148**, 155–191 (1984).

[2] A. Pumir, "A numerical study of pressure fluctuations in three-dimensional, incompressible, homogeneous, isotropic turbulence," Phys. Fluids **6**, 2071–2083 (1994).

[3] N. Cao, S. Chen, and G. Doolen, "Statistics and structures of pressure in isotropic turbulence," Phys. Fluids **11**(8), 2235–2250 (1999).

[4] T. Gotoh and R. Rogallo, "Intermittency and scaling of pressure at small scales in forced isotropic turbulence," J. Fluid Mech. **396**, 257–285 (1999).

[5] C. E. Brennen, *Cavitation and Bubble Dynamics* (Oxford University Press, 1995).

[6] K. Morch, "Cavitation inception from bubble nuclei," Interface Focus **5**, 20150006 (2015).

[7] M. Plesset, "The dynamics of cavitation bubbles," J. Appl. Mech. **16**, 277–282 (1949).

[8] S. Li, C. Brennen, and Y. Matsumoto, "Introduction for amazing (cavitation) bubbles," Interface Focus **5**, 20150059 (2015).

[9] S. Li, "Tiny bubbles challenge giant turbines: Three Gorges puzzle," Interface Focus **5**, 20150020 (2015).

[10] R. Arndt and W. George, "Pressure fields and cavitation in turbulent shear flows," in *Twelfth Symposium on Naval Hydrodynamics* (National Academy of Sciences, 1979), Technical Paper No. 91, Series A, pp. 327–339.

[11] S. Hilgenfeldt, M. Brenner, S. Grossmann, and D. Lohse, "Analysis of Rayleigh-Plesset dynamics for sonoluminescing bubbles," J. Fluid Mech. **365**, 171–204 (1998).

[12] B. Ran and J. Katz, "Pressure fluctuations and their effect on cavitation inception within water jets," J. Fluid Mech. **262**, 223–263 (1994).

[13] B. Belahadji, J. Franc, and J. Michel, "Cavitation in the rotational structures of a turbulent wake," J. Fluid Mech. **287**, 383–403 (1995).

[14] A. La Porta, G. Voth, F. Moisy, and E. Bodenschatz, "Using cavitation to measure statistics of low-pressure events in large-Reynolds-number turbulence," Phys. Fluids **12**, 1485–1496 (2000).

[15] E. Korkut and M. Atlar, "On the importance of the effect of turbulence in cavitation inception tests of marine propellers," Proc. R. Soc. London, Ser. A **458**, 29–48 (2002).

[16] J. Cardesa, A. Vela-Marín, and J. Jiménez, "The turbulent cascade in five dimensions," Science **357**, 782–784 (2017).

[17] Y. Li, E. Perlman, M. Wan, Y. Yang, R. Burns, C. Meneveau, R. Burns, S. Chen, A. Szalay, and G. Eyink, "A public turbulence database cluser and applications to study Lagrangian evolution of velocity increments in turbulence," J. Turbul. **9**, N31 (2008).

[18] H. Yu, K. Kanov, E. Perlman, J. Graham, E. Frederix, R. Burns, A. Szalay, G. Eyink, and C. Meneveau, "Studying Lagrangian dynamics of turbulence using on-demand fluid particle tracking in a public turbulence database," J. Turbul. **13**, N12 (2012).

[19] Forced isotropic Turbulence Dataset (Extended), https://doi.org/10.7281/T1KK98XB.

[20] S. Pope, *Turbulent Flows* (Cambridge University Press, 2000).

[21] P. Yeung, "Lagrangian investigations of turbulence," Annu. Rev. Fluid. Mech. **34**, 115–142 (2002).

[22] The relationship between the nondimensional variables chosen by Gotoh and Rogallo and those adopted here is $F_p = (4/9) \text{Var}(p)$.

[23] K. Goh and A. Barabási, "Burstiness and memory in complex systems," Europhys. Lett. **81**, 48002 (2008).

[24] J. Jiménez, A. Wray, P. Saffman, and R. Rogallo, "The structure of intense vorticity in isotropic turbulence," J. Fluid Mech. **255**, 65–90 (1993).

[25] B. Chen and M. Oevermann, "LES investigation with an Eulerian stochastic field cavitation model," in *Proceedings of the 10th International Symposium on Cavitation CAV2018*, edited by J. Katz (ASME, 2018), p. 05138.

[26] X. Lyu, X. Hu, and N. Adams, "Investigation of cavitation bubble cloud with discrete Lagrangian tracking," in *Proceedings of the 10th International Symposium on Cavitation CAV2018*, edited by J. Katz (ASME, 2018), p. 05123.

[27] K. Maeda and T. Colonius, "Eulerian-Lagrangian method for simulation of cloud cavitation," J. Comput. Phys. **371**, 994–1017 (2018).